

Flight Evaluation of Augmented Controls for Approach and Landing of Powered-Lift Aircraft

James A. Franklin,* Charles S. Hynes,† Gordon H. Hardy,‡
James L. Martin,‡ and Robert C. Innis§
NASA Ames Research Center, Moffett Field, California

Flight experiments were conducted with Ames Research Center's Quiet Short-Haul Research Aircraft to evaluate the influence of highly augmented control modes on the ability of pilots to execute precision instrument flight operations in the terminal area, particularly approaches to and landings on a short runway. The aircraft is a powered-lift, short-takeoff and landing configuration that is equipped with a modern digital fly-by-wire flight control system, a head-up display, and a color head-down display that make it possible to investigate control concepts and display format and content for full envelope, powered-lift operations. Considerable attention has been devoted in this flight program to assessing flightpath and airspeed command and stabilization modes developed using nonlinear, inverse model-following methods. The primary benefit of this control concept was realized when the pilot was required to execute a complex transition and approach under instrument conditions and in the presence of a wide range of wind and turbulence conditions. The concept and its design criteria have been defined to the point that is ready for consideration for aircraft design when warranted by mission requirements or complex control configurations.

Nomenclature

a_z	= normal acceleration
C_D	= drag coefficient
C_L	= lift coefficient
C_T	= thrust coefficient
F_c	= column force
g	= gravitational acceleration
h	= altitude
\dot{h}_c	= filtered vertical velocity
i_w	= wing incidence
K_{a_z}	= normal acceleration feedback gain
K_c	= column-force feedforward gain
K_{n_z}	= normal acceleration feedforward gain
K_T	= throttle feedback gain
K_v	= airspeed feedback gain
K_{vi}	= airspeed integral feedback gain
K_γ	= flightpath angle gain
$K_{\gamma\theta}$	= pitch attitude to flightpath-angle feedforward gain
m	= aircraft mass
\dot{m}	= engine mass flow rate
MSL	= altitude above mean sea level
N_2	= engine core speed
q	= free-stream dynamic pressure
q_B	= pitch rate
S	= wing area
s	= argument of Laplace transform
T_E	= engine response time constant
T_G	= gross thrust
U	= flightpath velocity
\dot{U}	= acceleration along flightpath
USB	= upper-surface blown flap

V_C, V_{CF}	= calibrated airspeed
V_S, V_{SF}	= selected airspeed
V_T	= true airspeed
W, GW	= aircraft gross weight
X	= axial force along flightpath
Z	= force normal to flightpath (positive downward)
α	= angle of attack
γ	= flightpath angle
δ_{AMB}	= standard atmosphere pressure ratio
δ_F	= outboard flap deflection
δ_{SP}	= spoiler deflection
δ_T	= throttle-lever position
δ_{USB}	= USB flap deflection
ζ	= damping ratio
Θ	= pitch attitude
θ_2	= standard atmosphere temperature ratio
Φ	= bank angle
ω	= frequency
ω_{WO}	= spoiler washout frequency

Subscripts

A	= air mass
C	= commanded
FA	= free air frame
M	= pilot's commands
o	= initial conditions (at engagement)
POT	= potential
RAM	= ram drag
USB	= upper surface blowing
WCR	= critical waypoint

Introduction

TACTICAL military operations from short fields and damaged runways impose stringent demands for precise control of flightpath and airspeed over an aircraft's low-speed flight envelope. These operations require the ability to perform a precision approach under instrument meteorological conditions (IMC) down to at least 100-ft ceilings and 1200-ft visual range, and to land in poor visibility in a touchdown zone as small as 200 × 50 ft. Control augmentation systems and cockpit displays that provide precision flightpath and airspeed control over the range of flight conditions and air-

Presented as Paper 85-1944 at the AIAA Guidance, Navigation and Control Conference, Snowmass, CO, Aug. 19-21, 1985; received April 21, 1986. This paper is declared a work of the U.S. Government and is not subject to copyright protection in the United States.

*Research Engineer, Flight Dynamics and Controls Branch. Associate Fellow AIAA.

†Research Engineer, Flight Dynamics and Controls Branch.

‡Research Pilot, Flight Operations Branch.

§Chief, Flight Operations Branch.

craft configurations can enable routine achievement of these demanding operations. Since future aircraft designed to provide this capability can be expected to incorporate features such as powered-lift, deflected thrust, and in-flight thrust reversing to achieve short-field performance and control precision, the ability to integrate these diverse controls will be crucial to the success of the control system design. To achieve good flying qualities for such a demanding task, this control precision must be provided without the need for the pilot to 1) compensate for deficiencies inherent in the response of the basic aircraft at these low airspeeds, 2) to manage the various individual control devices associated with such an aircraft configuration, or 3) to integrate separate instrument displays to maintain situation awareness.

To this time, efforts to provide the capability for these operations have been based on control-system concepts developed using linear fixed-operating-point methods and on flight director displays that provide commands for path tracking and for configuration management through transition from conventional to powered-lift flight. Concepts of this sort were devised and carried through flight evaluations on the NASA Augmentor Wing powered-lift research aircraft; design criteria for these systems were defined as well.¹⁻⁵ The work in Refs. 4 and 5 for flight director design and configuration management during transition was based on principles set forth in Ref. 6 from analyses and ground-based simulator experiments. In each of these cases, the desired precision of performance was achieved, with reasonable pilot effort, for curved, decelerating approaches under simulated instrument flight conditions, and satisfactory (Level 1) pilot ratings were obtained.

Related experience has been acquired from V/STOL aircraft control system and display investigations, particularly for the transition and instrument approach. Results of flight experiments on the X-22A^{7,8} and on the NASA CH-47B^{9,10} have demonstrated the ability to achieve Level 1 flying qualities for this task with systems based on linear, fixed-operating-point control concepts and with flight director guidance. Furthermore, ground-based simulation investigations of V/STOL operations using full-envelope model-following controls and flightpath-centered integrated command and situation displays, have received comparably good pilot ratings for a curved, decelerating approach on instruments to a visual shipboard landing.^{11,12}

The experience noted above has proved the feasibility of performing successfully such demanding flight operations with powered-lift aircraft. The objective of the work reported in this paper was to assess entirely different approaches to control system design for a similar operational application. There was particular interest in a control system concept that employs the aircraft's nonlinear aerodynamics explicitly as a functional element in the system. Conventional design practice uses feed-forward and feedback gains determined from linear analyses about fixed operating points, and scheduled to account for varying flight conditions and aircraft configuration. The required complexity of this gain scheduling to accommodate a large flight envelope including significant aerodynamic nonlinearities, influenced by several parameters and configuration variations, is a disadvantage of this design approach. The full-envelope flightpath and airspeed command and stabilization system developed for use in these evaluations was based on the nonlinear, inverse model-following concept.¹³⁻¹⁵ An investigation of electronic head-up and color head-down primary flight displays was conducted in conjunction with the flight control concept evaluation. These displays are flightpath centered, and are intended to take advantage of inertial reference system accuracy, electronic display flexibility, and currently available computational capability. They provide command and status information in an integrated format intended to heighten situation awareness for terminal operations while enabling tracking performance as precise or better than that obtained with flight director

guidance. Principles of the display concepts and results of their evaluation are presented in Ref. 16.

Experiments have been conducted on simulators at Ames Research Center and on the Quiet Short-Haul Research Aircraft (QSRA) to provide pilot evaluations of this control concept for instrument approaches and landings. The influences on the precision of approaches and landings and on the effort pilots must devote to executing these demanding operations have been defined. The material that follows in this paper describes the principles of the control system, the flight experiments and the powered-lift research aircraft (QSRA) on which they were conducted, and the findings which were obtained from these experiments.

Description of Research Aircraft

The research aircraft on which these flight experiments were conducted is a four-engine, powered-lift jet transport (Fig. 1) that uses an upper-surface-blown (USB) flap propulsive-lift system. The basic airframe is a deHavilland C-8A Buffalo, which was modified by the Boeing Company to incorporate an integrated wing and propulsion system, including AVCO Lycoming YF-102 turbofan engines.^{17,18} The primary flight controls consist of a single-segment elevator for pitch control, ailerons and spoilers for roll control, and a two-segment rudder for yaw control. In addition, flap segments aft of the engines, the USB flaps, are used to modulate lift and drag throughout the aircraft's powered-lift envelope. The spoilers may also be used for lift and drag control.

The aircraft's basic powered-lift aerodynamics and installed thrust are sufficient to provide a performance envelope at low airspeed that exceeds those of modern transport or fighter aircraft in terminal operating conditions, and those of any proposed advanced designs as well. Figure 2 illustrates the QSRA climb and descent capability at low speed in comparison to

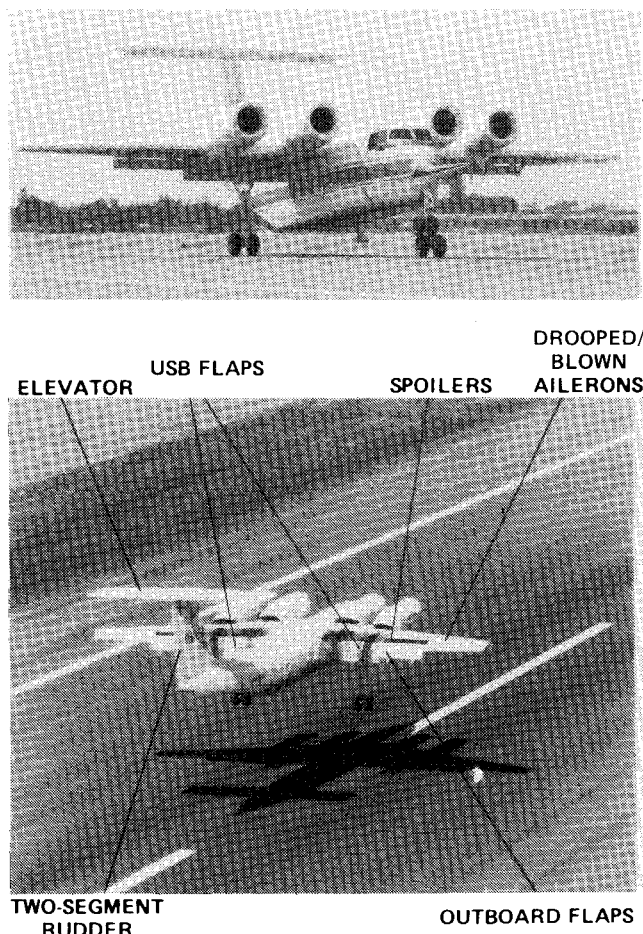


Fig. 1 Quiet short-haul research aircraft.

past or present transports (e.g., YC-14 and 15) and conceptual fighter configurations, such as the STOL and Maneuver Technology Program aircraft now under development. Flightpath and airspeed control authority provided by the full range of thrust settings, flap and spoiler deflections, and angle of attack are substantial; the challenge is to integrate these controls so as to manage the aircraft configuration and to provide the dynamic response to the pilot's commands necessary to achieve good flying qualities over this large flight envelope.

Flap and spoiler controls are fully fly-by-wire over their range of authority. For research operations, USB flap authority is restricted to the range from 15 deg to full flap deflection of 66 deg; spoiler authority is restricted to 0 to 30 deg. Series electrohydraulic actuators also provide limited authority commands to the pitch, roll, and yaw control surfaces. The throttle handles may be driven by electromechanical parallel actuators connected to the throttles through slip clutches. All of the electrically actuated controls are driven by a digital computer, which accepts control commands from the pilot and inputs from the aircraft's motion sensors, and generates appropriate commands for the control actuators.¹⁹ This system also drives the cockpit electronic displays to provide guidance and control commands to the pilot.

Augmented Flight Control and Display Concepts

Flight Control System

Attitude Stabilization and Command Augmentation System

To achieve good flightpath control, it is generally accepted that it is necessary to have good attitude control characteristics. In the case of the QSRA, the basic aircraft's pitch, roll, and yaw response characteristics are representative of the class of low-speed, powered-lift aircraft (e.g., Ref. 4) and consist of poor longitudinal stability and large trim changes owing to thrust and flap variations, low yaw damping, and adverse yawing moments because of lateral controls and rolling velocity. To improve the basic aircraft's pitch, roll, and yaw response, stabilization and command augmentation modes were developed based on currently available criteria and conventional response feedback control. These control modes have a high degree of similarity to those described in Ref. 4. Rate-command/attitude-hold features were provided for pitch and roll control and were designed to a control bandwidth of 2-2.5 rad/s. Bandwidth is based on the lowest open-loop attitude response frequency for which either a minimum of a 45-deg phase margin or a 6-dB gain margin is provided. Turn coordination and Dutch roll damping were included in the yaw axis, designed to standards set by MIL-F-8785C for sideslip suppression, Dutch-roll damping ratio, and roll-rate oscillations. Based on the pilots' evaluations of a similar system for the powered-lift aircraft in Ref. 4, these modes were expected to, and did, produce satisfactory pitch attitude, bank angle, and heading control.

Flightpath and Airspeed Stabilization and Command Augmentation

To permit control of flightpath and airspeed throughout the aircraft's powered-lift envelope, the USB flaps, throttles, and spoilers were driven by a command structure that was based on nonlinear, inverse model-following system concepts. A diagram of the system structure is presented in Fig. 3. Essential features are the input commands, the feedback regulator, nonlinear trim maps, and the control actuator commands. As shown in the figure, the pilot's inputs and the feedback regulator outputs combine to form commanded accelerations in the longitudinal and vertical axes. These accelerations are converted to commanded lift and drag coefficients based on the aircraft's weight and flight condition, and are used as inputs, along with angle of attack, to the trim maps. These maps, which are the heart of the system, convert the commanded lift and drag coefficients into the commanded surface positions and thrust that will produce the desired accelera-

tions. Thus, the feedback regulator acts through the trim maps and aircraft dynamics in cascade, which in effect has been transformed into a linear, constant-coefficient system. Consequently, effects of aircraft configuration and flight condition are incorporated in the trim maps; and it is unnecessary to schedule gains to account for these influences. The desired flightpath dynamic response is achieved throughout the aircraft's flight envelope without small-perturbation restrictions, and, perhaps most important, the designer retains a direct physical appreciation of the effects of the aircraft's aerodynamics on its dynamic response.

To be more specific about the functions of the trim maps, of the model commands, and of the feedback or regulator loop, the equations defining the system, based on the assumption of coordinated flight and derived in a flight-path-oriented axis system with respect to the air mass, are presented as follows. The equations that are used to define the trim maps are nothing more than the equations of motion for axial and normal force, and the objective is to determine the control positions and engine thrust that will produce the axial and normal accelerations that will satisfy the pilot's commands and the feedback regulator demands. The detailed system block diagram in Fig. 4 may be used as an aid in their interpretation. Given the equation for axial or streamwise force

$$m\dot{U} = X - W\sin\gamma \quad (1)$$

the total aerodynamic and propulsive force required to achieve the desired axial acceleration \dot{U} is

$$X = m\dot{U}_c + W\sin\gamma_M \quad (2)$$

$$= -C_D q S \quad (3)$$

where the total drag or streamwise force coefficient, as measured on a wind-tunnel balance, includes combined airframe-thrust and ram-drag components. When the ram-drag contribution is removed, the remaining propulsion-influenced aerodynamic component is

$$C_{DFA} = C_D - C_{DRAM} \quad (4)$$

where the engine inlet momentum drag is

$$C_{DRAM} = \frac{\dot{m}U}{qS} \quad (5)$$

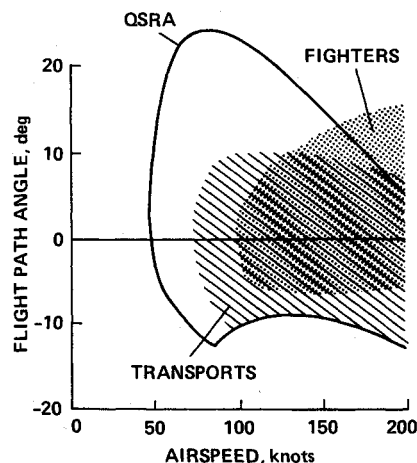


Fig. 2 QSRA performance.

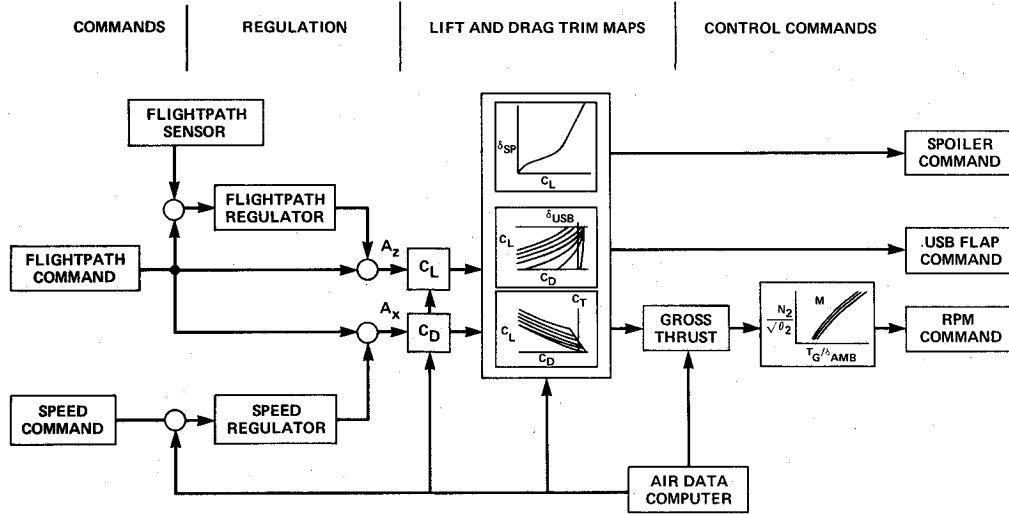


Fig. 3 Nonlinear inverse concepts for flightpath and airspeed command and augmentation systems.

The required airframe drag coefficient (including thrust) can be defined as

$$C_{DFA} = -\frac{W/S}{q} \left[\frac{\dot{U}_c}{g} + \sin \gamma_M \right] - \frac{mU}{qS} \quad (6)$$

From the equation for normal force

$$mU\dot{\gamma} = -Z - W \cos \gamma \quad (7)$$

where the total force required to achieve the desired acceleration ($U\dot{\gamma}$) normal to the flightpath is

$$Z = -mU\dot{\gamma}_c - W \cos \gamma_M \quad (8)$$

$$= -C_L q S \cos \Phi \quad (9)$$

Thus, the required total airframe lift coefficient, including propulsion-induced lift is

$$C_L = \frac{W/S}{q \cos \Phi} \left[\frac{U\dot{\gamma}_c}{g} + \cos \gamma_M \right] \quad (10)$$

For this aircraft, drag and lift coefficients have the general functional relationships

$$C_{DFA} = f(\alpha, C_T, \delta_{USB}, \delta_{SP}, \delta_F) \quad (11)$$

$$C_L = g(\alpha, C_T, \delta_{USB}, \delta_{SP}, \delta_F) \quad (12)$$

that include the parametric influences of angle of attack and thrust coefficient and the configuration variables USB flaps, spoilers, and outboard flaps. However, the redundancy in these relationships can be eliminated by appropriate choices defining outboard flaps, spoilers, and angle of attack as dependent variables. Since the outboard flaps are virtually independent of powered-lift effects, they are selected to their fully deflected position before commencing powered-lift operation. Spoilers are deployed to a nominal bias position to permit them to be used to quicken lift response, as will be discussed shortly. Angle of attack is determined by pitch attitude and flightpath angles ($\alpha = \Theta - \gamma_A$). With this reduction in the number of independent variables from which to determine drag and lift

$$C_{DFA} = f(C_T, \delta_{USB})_{\alpha, \delta_{SPB}, \delta_F} \quad (13)$$

$$C_L = g(C_T, \delta_{USB})_{\alpha, \delta_{SPB}, \delta_F} \quad (14)$$

Since lift generation requires dynamic response that is beyond the capability of the engines or USB flaps, the spoilers are employed in the short term to produce incremental lift quickly, then are restored to their nominal bias position by washing out the initial lift command. Therefore, the functional relationship for lift coefficient is

$$C_L = g_1(C_T, \delta_{USB})_{\alpha, \delta_{SPB}, \delta_F} + g_2(\delta_{SP}) \quad (15)$$

With both lift and drag determined by two independent controls it is possible to define a unique relationship to calculate the required thrust and USB flap that will yield the commanded lift and drag coefficients. Thus the trim maps used to compute thrust coefficient and USB flap are described by

$$C_T = f(C_{DFA}, C_L)_{\alpha, \delta_{SPB}, \delta_F} \quad (16)$$

$$\delta_{USB} = g(C_{DFA}, C_L)_{\alpha, \delta_{SPB}, \delta_F} \quad (17)$$

The required spoiler is

$$\delta_{SP} = f(C_L) \left(\frac{s}{s + \omega_{WO}} \right) \quad (18)$$

where $f(C_L) = f(C_L - C_L(\alpha))$, and the washout is selected to complement the engine thrust time constant ($\omega_{WO} = 1/T_E = 1.0$ s).

Gross thrust and eventually engine power setting are computed from thrust coefficient, where

$$T_G = C_T q S \quad (19)$$

Corrected engine core speed is, in turn, related to corrected gross thrust and Mach number,

$$\frac{N_2}{\sqrt{\theta_2}} = f \left(\frac{T_G}{\delta_{AMB}}, \text{Mach} \right) \quad (20)$$

and is converted to a position command for the throttle position servo.

The trim maps described in the foregoing discussion accommodate a generalized command and feedback structure. For the system selected for evaluation, the pilot's commands and the response feedbacks that combine to provide the normal and axial acceleration commands to the trim maps are as follows. For flightpath control, a combination of acceleration command and feedback and flightpath angle command and

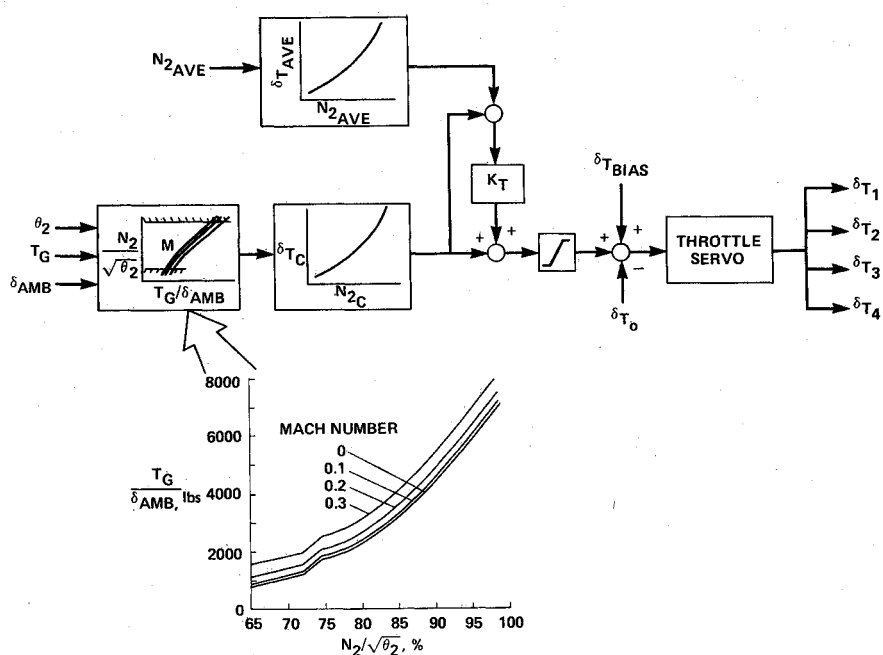
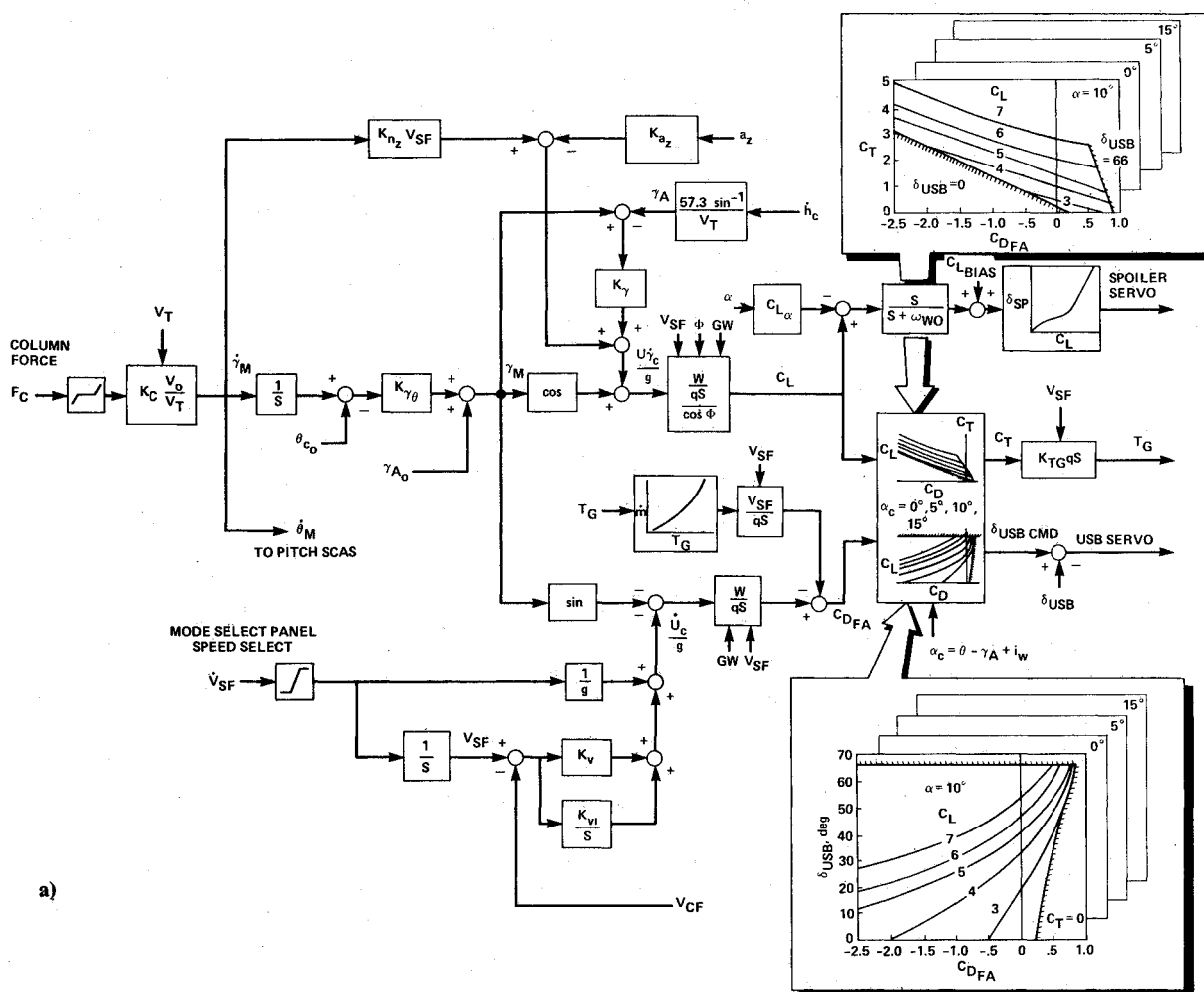


Fig. 4 System block diagrams: a) flightpath-airspeed command and augmentation system; b) thrust command system.

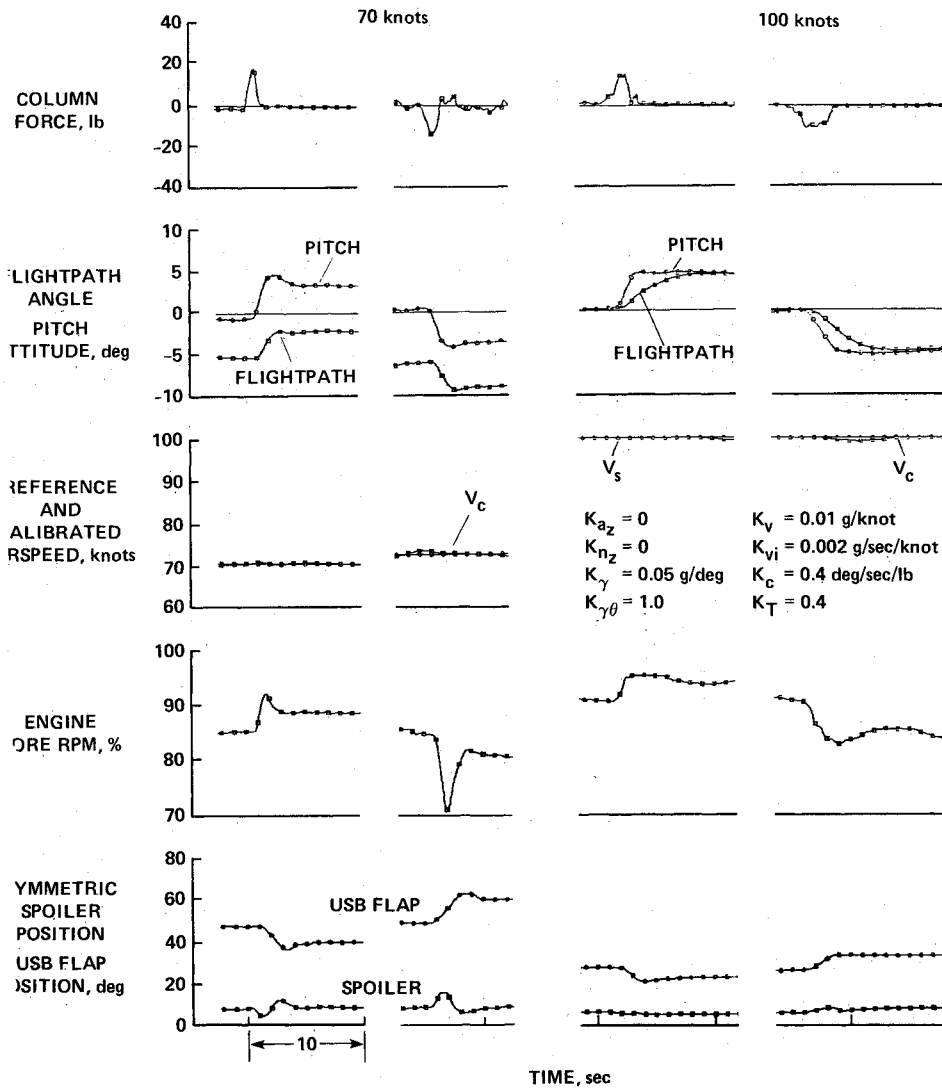


Fig. 5 Examples of transient response to the pilot's longitudinal control.

feedback combine as follows:

$$\frac{U\dot{\gamma}_c}{g} = K_{n_z} V_{SF} \dot{\gamma}_M - K_{a_z} a_z + K_\gamma K_{\gamma\theta} \gamma_M - K_\gamma \gamma \quad (21)$$

The flightpath command is generated in accord with a front-side control technique, in which flightpath is controlled by modulating the aircraft's pitch attitude. In this case, commanded flightpath rate $\dot{\gamma}_M$ and commanded pitch rate $\dot{\theta}_M$ are equivalent:

$$\begin{aligned} \dot{\gamma}_M &= (K_c V_0 / V_T) F_c \\ &= \dot{\theta}_M \end{aligned} \quad (22)$$

Dynamic response of flightpath and pitch attitude are different, of course, and are based on their respective feedback regulator gains. For speed control, the command and regulator equation is

$$\frac{\dot{U}_c}{g} = \frac{\dot{V}_{SF}}{g} + \left(K_v + \frac{K_{vi}}{s} \right) (V_{SF} - V_{CF}) \quad (23)$$

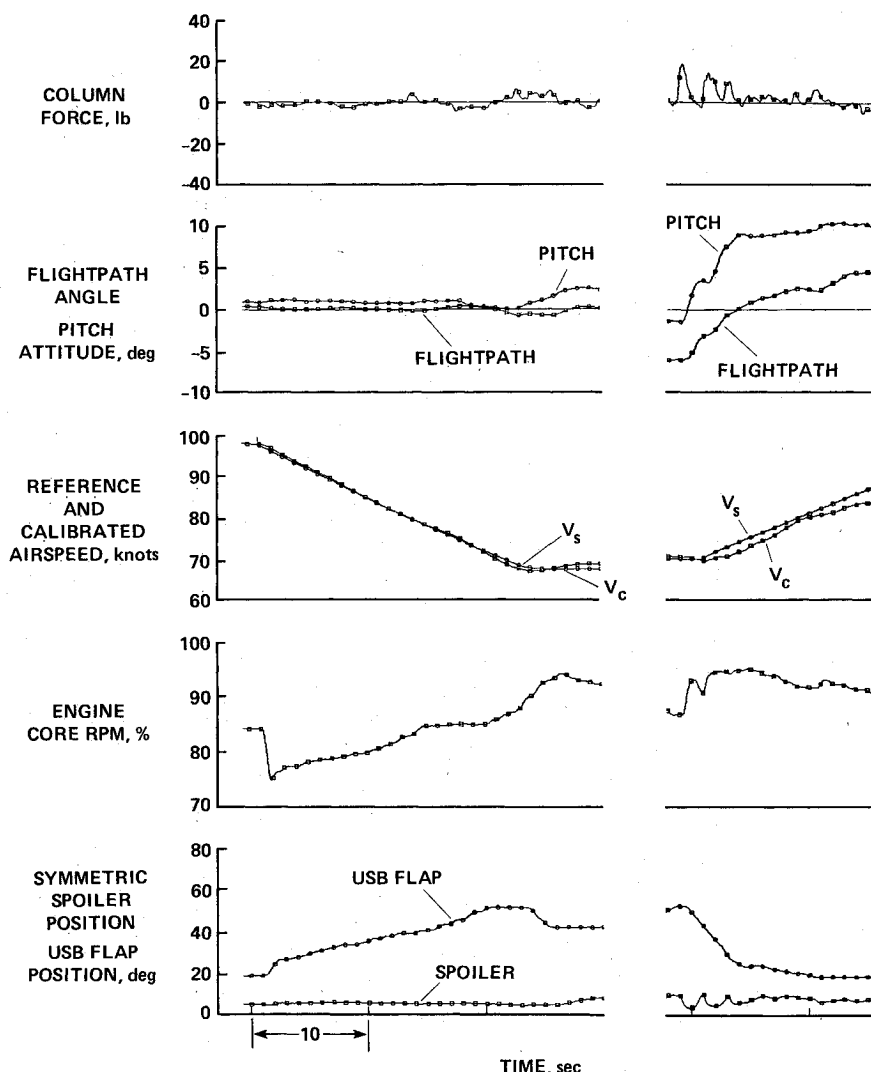
From these equations, the transfer function for flightpath response to the pilot's control input, assuming no aerodynamic model errors and high bandwidth control servo

response is

$$\frac{\dot{\gamma}}{F_c} = \left(\frac{K_c K_{\gamma\theta} V_0}{V_T} \right) \frac{\left[\frac{K_{n_z} V_{SF}}{K_\gamma K_{\gamma\theta}} s + 1 \right]}{\left[\frac{1 + K_{a_z}}{K_\gamma / V_T} s + 1 \right]} \quad (24)$$

Control sensitivity for both pitch attitude and flightpath model commands to control force is determined by K_c , and the ratio of flightpath-to-pitch-attitude-response in the steady state is controlled by $K_{\gamma\theta}$. Control sensitivity varies as the inverse of airspeed to maintain constant normal acceleration response to the control. In the absence of acceleration command feedforward (K_{n_z}) or feedback (K_{a_z}), flightpath response bandwidth is established by the time-constant V_T / K_γ . When feed-forward and feedback acceleration information is used to provide lead-lag compensation, flightpath bandwidth can be extended beyond that provided by flightpath-angle feedback alone. The flightpath control system was designed to provide a flightpath bandwidth of 0.8 to 1.0 rad/s for approach speeds of 60 to 70 knots. Flightpath response sensitivity of 0.4 deg/s/lb and a one-to-one ratio of flightpath-to-pitch attitude was selected, based on the results of Ref. 4. The speed-select command \dot{V}_{SF} is limited to provide appropriate acceleration and deceleration levels associated with various regions of the flight envelope. Airspeed stabilization was designed to a bandwidth of 0.2 rad/s to reject tur-

Fig. 6 Examples of transition between powered-lift and cruise flight.



bulence inputs while retaining authority to suppress lower-frequency shear disturbances.

It should be noted that angle-of-attack trim capability is provided by allowing pitch attitude to be changed independent of the flightpath command. This trim can either be performed by the pilot or by an automated trim logic used for configuration control during transition.

The diagrams in Fig. 4 serve to illustrate the overall command, regulation, trim map, and control output structure of the system. Command inputs originate from the pilot's longitudinal control force and the glare-shield-mounted mode-select panel. Flightpath and airspeed feedback to their respective regulators are derived from complementary filters. Examples of the trim maps for computation of thrust coefficient and USB flap are shown in the insets to Fig. 4 for an angle of attack of 10 deg. These trim maps are also supplied for angles of attack of 0, 5, and 15 deg; the computation of thrust coefficient and USB flap deflection is accomplished using a three-variable table look-up procedure. For example, at a wing loading of 83 lb/ft², an approach speed of 70 knots, an approach-path angle of -6 deg, and an angle of attack of 10 deg, the required lift and drag coefficients (after accounting for ram drag) are $C_L = 5$, $C_{DFA} = 0.23$. With these independent variables, it may be seen from the trim map insets in Fig. 4 that the corresponding thrust coefficient and USB flap deflection are $C_T = 1.25$ and $\delta_{USB} = 46$ deg, respectively. These tables and the data relating corrected gross thrust to corrected engine core speed were obtained from large-scale wind-tunnel model and engine test-stand data.²⁰

The computer that contains the flight control software incorporates a processor adapted from a flight guidance computer used in commercial transport aircraft. The memory required to accommodate the flightpath-airspeed SCAS is 2000 words; this portion of the software executes in 5 msec. For comparison, the conventionally designed pitch, roll, and yaw SCAS requires 1800 words and is executed in 4 msec.

Representative time-response characteristics of the flightpath-airspeed command and stabilization system selected from flight data are presented in Figs. 5 and 6 to illustrate the aircraft's response over its powered-lift envelope. Responses to commanded changes in flightpath at 70 and 100 knots are shown in Fig. 5. Flightpath responds crisply to the pilot's column force command with time-constants of flightpath response between the low- and higher-speed conditions that vary in proportion to airspeed. Engine rpm, USB flap, and spoiler activity appear to be modest, and the spoiler washout is evident. The behavior of the system during transitions between 70 and 100 knots is shown in Fig. 6. The transitions are smooth, with no appreciable speed lag and little overshoot. Very little perturbation in pitch attitude or flightpath occurs while executing the deceleration. Engine thrust setting and flap position are managed smoothly as the transition progresses. The accelerating, climbing transition shown in Fig. 6 is representative of a go-around maneuver. During the latter stages of the acceleration, the USB flap reaches the upper limit of 15 deg imposed by the digital fly-by-wire system. At that point, the pilot must reduce angle of attack or flightpath angle in order for the transition to proceed to higher speeds.

Dynamic pressure (q) is computed based on commanded airspeed (V_{SF}) and standard sea-level air density. Temperature and pressure ratios were obtained from standard air data computations. Limits were imposed on speed regulation commands to the controls during the landing flare to permit a normal speed bleed-off during this maneuver. Integral speed-error commands were frozen when USB flap limits were encountered, unless these commands would serve to drive the flaps off their limits. Protection of operating envelope limits in accord with the criteria of Ref. 21, particularly those associated with angle-of-attack margins that ensure safe encounter with vertical gusts, are provided by limiting the angle-of-attack envelope to 15 deg. Lift margins associated with airspeed are protected by defining the reference speed appropriate to the flight condition and aircraft configuration.

Electronic Displays

For the reader to appreciate fully the contribution of these augmented control concepts to the overall closed-loop control of the aircraft, it is necessary to provide a brief description of the role of the displays in the QSRA. The displays are based on the principle that they should present cues normally available during visual flight so as to make the pilot's interpretation instinctive and to eliminate the need for flight-director-type commands. They provide path cues which the pilot normally extracts from the visual scene, effectively reducing instrument approach conditions to their quasi-visual counterparts. Under visual conditions, aircraft handling should be satisfactory to the pilot, either naturally or with the aid of control augmentation.

The essential features of both the head-up display (HUD) and head-down display are illustrated in Fig. 7. Eulerian attitude angles, derived from an inertial reference system, and a perspective runway, derived from ground-based guidance, are displayed conformally by the HUD (see horizon line with heading tape, airplane symbol, pitch scale, and roll attitude and indices). A glide-slope reference line displays the selected glide slope, and a fixed line indicates the maximum safe downward flightpath. A moving aircraft symbol represents a lead (ghost) which flies a perfect approach a few seconds ahead on the selected path. The flightpath symbol, derived from ground-based guidance data complemented with inertial acceleration, is central to the display. The flightpath symbol group comprises the airspeed error tape, the flightpath acceleration symbol (chevron), the flightpath acceleration command symbol (bucket), and digitally displayed radio altitude and calibrated airspeed. A caution or warning symbol (not shown) alerts the pilot to unannounced messages. All these symbols of the flightpath group move together over the display, maintaining a fixed relationship. The use of pictorial elements wherever possible in preference to scales or digits contributes to the simplicity and uncluttered appearance of the display.

The pilot's task is to fly in loose formation with the lead aircraft by placing the flightpath symbol on the ghost symbol. The ghost symbol is driven relative to the runway symbol by scaled localizer and glide-slope errors, and provides a direct indication of these errors. Thus the ghost, runway, and flightpath symbols combine to form a pursuit display which integrates command with situation information, instead of presenting the command in isolation as a compensatory flight director does. For example, Fig. 7 illustrates a representative situation at the 100-ft decision height. The position of the runway touchdown zone (heavy stripes) slightly above the 6-deg glide-slope reference line shows that the aircraft is slightly below the glide slope. It is to the right of the runway centerline in a 6-deg left bank. The ghost therefore appears above the 6-deg glide-slope reference line and to the left of runway centerline. The flightpath symbol predicts that in the absence of path correction the aircraft would fly into the ground short of the runway threshold. Airspeed is 3 knots fast relative to the selected 70-knot reference speed (displayed on the mode-

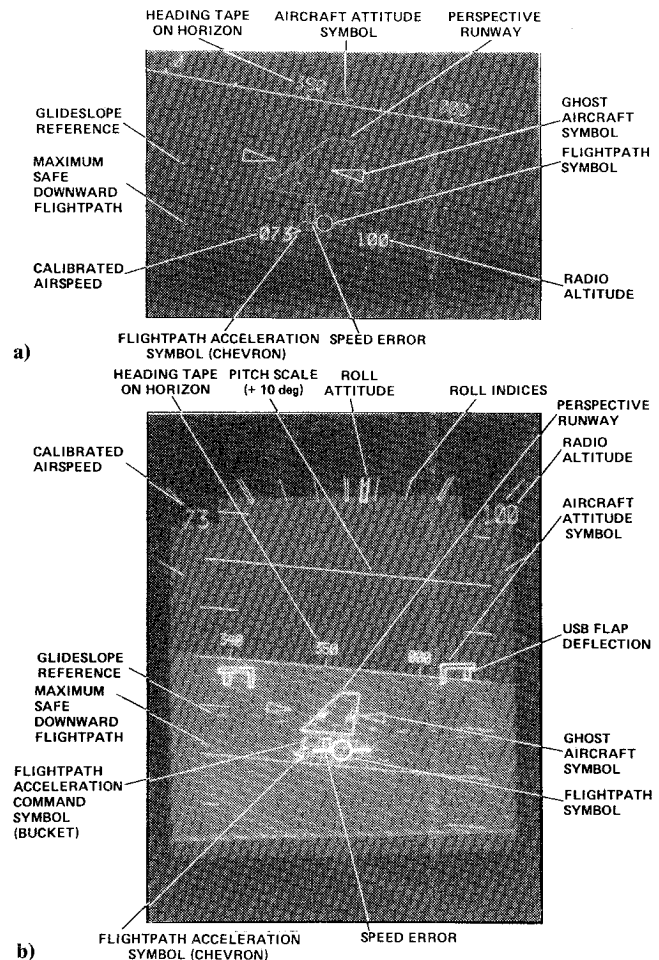


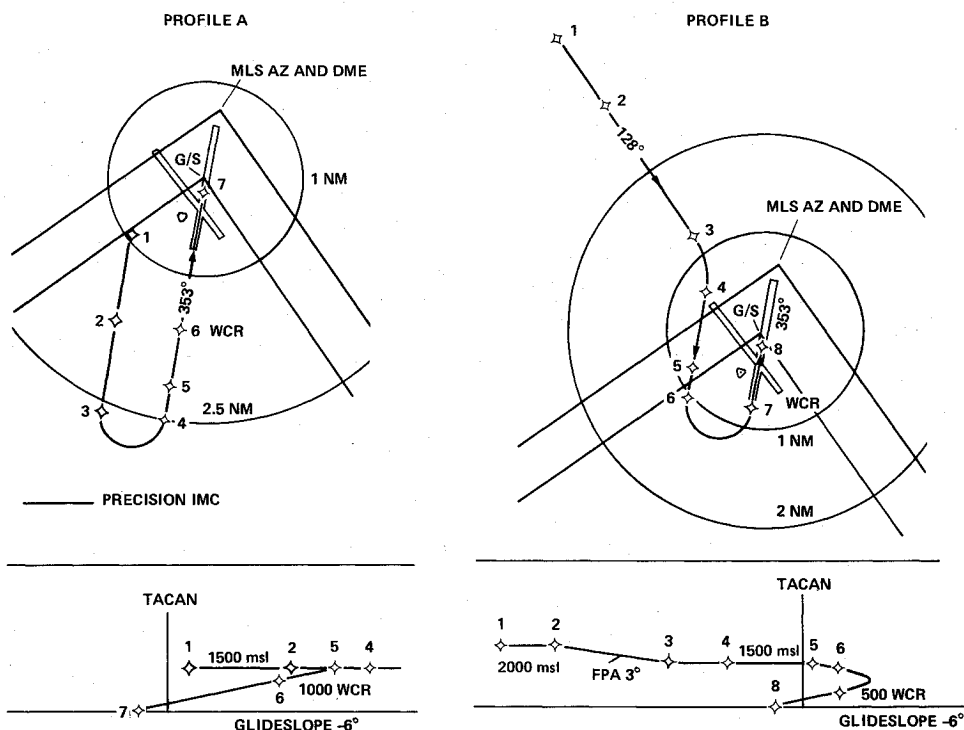
Fig. 7 Electronic primary flight displays: a) head-up display; b) head-down display.

select panel), and the aircraft is decelerating slightly (chevron below flightpath symbol). To correct these errors, the pilot must continue his left turn to center the flightpath symbol laterally on the ghost, fly a shallower flightpath in order to center the flightpath symbol vertically on the ghost, and decelerate to align the flightpath symbol with the bucket.

Description of Flight Experiments

Flight evaluations were conducted of transitions and approaches for two curved profiles (Fig. 8) that varied substantially in regard to the attention and effort that were required of the pilot. These approach paths consisted of left-hand patterns, the easier of which involved entering the downwind leg with the aircraft in the cruise configuration, reconfiguring for powered lift by deploying the USB flaps, capturing the localizer in level flight at the pattern altitude of 1500 ft and then acquiring the glide slope (profile A). Deceleration to final approach speed was performed either at glide-slope intercept or during the initial stage of the approach. A more challenging approach (profile B) required the pilot to execute a descending turn within 1 n.mi. of the runway, to decelerate during the turn to final approach speed, and to acquire the final straight-in segment at an altitude of 500 ft. Profile B was selected to provide the pilot a task representative of approaches along time- or fuel-conservative trajectories synthesized in real time,²² or tactical military operations against which advanced control and display concepts could be evaluated. All approaches were made on a 6-deg glide slope under simulated instrument conditions to a decision height of 100 ft in the wind conditions of the day. Approach guidance was provided by an MLS and by TACAN when out of MLS coverage. A final

Fig. 8 Reference flight trajectories for transition and approach.



visual segment was flown to landing on a 100×1700 -ft runway with a designated touchdown zone 200 ft in length positioned 300 ft from the runway threshold.

Four NASA research pilots participated in this flight program. Pilot ratings and commentary were obtained for control-display combinations that built up from the basic aircraft with raw data guidance to the full flight-path-airspeed command augmentation system with electronic head-up and head-down displays. The raw data presentation consisted of attitude and vertical speed in analog form and airspeed and altitude in digital form on the PFD, along with heading, localizer, and glide-slope deviations provided on a conventional horizontal-situation indicator. Evaluations were made of intermediate configurations that only provided attitude augmentation with and without the electronic displays. Configurations were paired to permit the independent assessment of improvement in controls and displays; thus, attitude and flight-path-airspeed augmentation systems were evaluated with the electronic displays, and raw data and electronic displays were evaluated with attitude augmentation.

Discussion of Results

Transition and Approach Evaluations

Results of the pilots' evaluations for the transition and approach to decision height are shown in Fig. 9. Cooper-Harper ratings illustrate the trends in flying qualities for the IMC approach for the control-display combinations. Each data point represents the evaluation of an individual pilot, and is based on experience accumulated from several approaches. Data are shown for essentially calm winds and for strong crosswinds with light to moderate turbulence for profile A. These evaluations indicate the potential for improving precision approach control through the use of control augmentation and electronic displays. The basic aircraft with raw data display presentation is considered to be marginally adequate for executing the instrument approach, and the operational minimum decision height for this configuration is restricted to 200 ft. The basis for the pilots' evaluations is the excessive effort required to track the localizer while maintaining reasonably coordinated flight and to maintain airspeed in the presence of the throttle and flap activity associated with performing the transition and tracking the glide slope. Factors in-

fluencing this critique are the aircraft's poor Dutch roll damping, sideslip excitation from the lateral controls, trim changes owing to thrust and flap, and the concentration required for the instrument scan. The provision of control augmentation for the pitch, roll, and yaw axes (attitude SCAS) improves those aspects of the aircraft's control so that the approach flying qualities are clearly adequate; nevertheless, considerable effort may still be required of the pilot to perform the transition, for speed control, and for the instrument scan. These results are comparable to evaluations obtained for a similar configuration in Ref. 4.

To achieve satisfactory flying qualities, it was necessary to use the electronic displays in combination with the pitch, roll, and yaw augmentation modes. The combination of precision guidance and a well-integrated format of situation information reduced the demands of the instrument scan to a minimum. Pilots rated tracking performance and the attention required to perform the task to be comparable to that associated with a conventional flight director approach, and the results correspond to evaluations of a three-axis flight director configuration from Ref. 4. Glide slope and localizer tracking accuracy was consistently within the Category II window at breakout. Finally, when the full-envelope flightpath-airspeed augmentation system was used for the transition and approach, demands on pilot effort and attention were minimized, and the associated flying qualities were assessed to be fully satisfactory. In calm winds, the improvement in flying qualities for the flightpath-airspeed augmentation over the attitude-augmentation modes is hardly significant. However, the flightpath-airspeed system serves to desensitize the aircraft to the influence of winds and turbulence; hence, the improvement offered by this system over attitude augmentation alone is more apparent as the intensity of the disturbances increases. In moderate turbulence, flying qualities degrade to adequate-marginally satisfactory for the attitude-augmentation system, whereas the flightpath-airspeed system is hardly affected. One pilot objected to the requirement to adjust angle of attack through the transition and rated this system somewhat more poorly than the other pilots did. Automation of the angle of attack trim removed this objection, and the system was rated satisfactory by all pilots. The pilot evaluations agree with those obtained from Ref. 4 for a flightpath-airspeed-

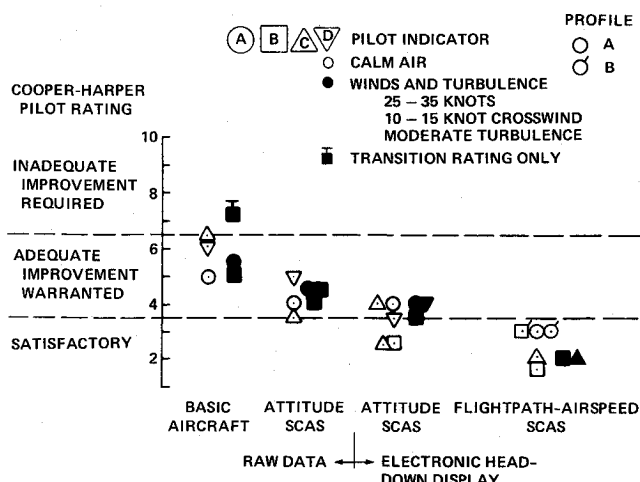


Fig. 9 Flying qualities evaluation of control-display modes for IMC transition and approach.

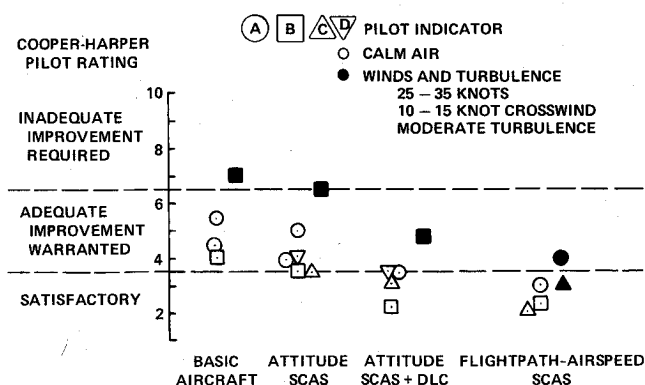


Fig. 10 Flying qualities evaluation of control modes for flare and landing.

augmentation system used in conjunction with a two-axis flight director. The adverse influence of turbulence is amplified when the approach must be flown on raw data guidance or without the aid of control augmentation. The basic aircraft is considered marginally adequate to inadequate for performing the instrument approach in turbulence.

Flight evaluations performed for profile B show that the advantage of flightpath and airspeed command and stabilization is most apparent when the pilot must perform a tight, curved decelerating approach. Based on the findings of the flight experiments of Refs. 1 and 4, electronic displays or flight directors and, at least, attitude augmentation are essential if flying qualities are to be adequate for executing the approach on a curved path such as that of profile B. For such a demanding maneuver, which may typify operations from short fields or from damaged runways, the aircraft is considered inadequate unless it is equipped to a standard at least this high. With the flightpath airspeed SCAS, this profile can be flown with satisfactory flying qualities providing the angle-of-attack trim is automated. For this SCAS mode, the pilots found that Profile B required very little more effort on their part than Profile A, because of the ease and precision of flightpath control and configuration management and the ability to readily assess the progress of the transition and approach along the most demanding profile.

Flare and Landing Evaluations

Data from the pilots' evaluations of the influence of control modes on the final visual approach segment to the runway and for the flare and landing are provided in Fig. 10. Individual pilot ratings are based on experience gained from several land-

ings for each configuration. Data were obtained in calm wind conditions and in winds up to the crosswind operating limit of the aircraft. During the final visual segment preceding the flare the pilot aligned the aircraft with the runway centerline and aimed for a point on the runway just short of the touchdown zone. The flare was executed to carry the aircraft into the zone and to reduce the sink rate. The pilots' assessments of their ability to perform this task were based on their ability to land consistently in the zone, with sink rates consistently in the range of 3 to 5 ft/s. The basic aircraft was considered to be adequate, a result of sluggish heave response to thrust and pitch attitude control and poor lateral-directional dynamics, all of which required the pilot to use considerable effort to align the aircraft laterally and to keep the touchdown within the zone. Incorporation of attitude augmentation improved the lateral-directional control and produced a slight improvement in the pilots' ratings; however, sink-rate control was still poor because of the sluggish response to throttles. The results are in accord with those of similar configurations presented in Refs. 1, 4, and 23. Improvements in heave response were made by integrating direct-lift control with the thrust control to obtain higher bandwidth sink-rate response than was provided by the basic airframe heave dynamics and the thrust response to throttles. With the improvements associated with this system, the landing task was considered to be at least marginally satisfactory. Ratings of the flightpath and airspeed command augmentation system indicate that it is fully satisfactory, though only a slight improvement over the integrated direct-lift throttle mode. Similar evaluations were obtained for systems of these types reported in Refs. 1 and 4. In the presence of strong winds and light-to-moderate turbulence, the basic aircraft was rated only marginally adequate, whereas the integrated direct-lift mode and flightpath-airspeed SCAS were rated only slightly worse than for calm conditions.

Concluding Remarks

This paper has described a flight experiment conducted with Ames Research Center's Quiet Short Haul Research Aircraft to evaluate the influence of highly augmented control modes on precision instrument flight operations in the terminal area, particularly approaches to and landings on a short runway. The primary benefits of these controls were realized when the pilot was required to execute precisely a complex transition and approach under instrument conditions and in the presence of a wide range of wind and turbulence conditions. Based on the results of this flight program, a flightpath and airspeed command and stabilization system that incorporates nonlinear, inverse systems concepts produced fully satisfactory flightpath control throughout the aircraft's terminal operating envelope; moreover, the system relieved the pilot of the need to manage the aircraft's configuration throughout the transition or to account for varying winds. Both the control concept and design criteria for it have been refined to the point that it is ready for consideration for future aircraft designs that must provide for demanding mission requirements or complex control configurations. Its use in civil aviation may be justified by the economic benefits of fuel or time-conservative trajectories.

References

- ¹Hindson, W.S., Hardy, G.H., and Innis, R.C., "Flight-Test Evaluation of STOL Control and Flight Director Concepts in a Powered-Lift Aircraft Flying Curved Decelerating Approaches," NASA TP-1641, March 1981.
- ²Hindson, W.S., Hardy, G.H., and Innis, R.C., "Flight Experiments Using the Front-Side Control Technique during Piloted Approach and Landing in a Powered-Lift STOL Aircraft," NASA TM-81337, April 1982.
- ³Hindson, W.S., "Analysis of Several Glidepath and Speed Control Autopilot Concepts for a Powered-Lift STOL Aircraft," NASA TM-84282, Aug. 1982.

⁴Franklin, J.A., Innis, R.C., and Hardy, G.H., "Flight Evaluation of Stabilization and Command Augmentation System Concepts and Cockpit Displays during Approach and Landing of a Powered-Lift STOL Aircraft," NASA TP-1551, Nov. 1980.

⁵Franklin, J.A., Innis, R.C., and Hardy, G.H., "Flight Evaluation of Configuration Management System Concepts during Transition to the Landing Approach for a Powered-Lift STOL Aircraft," NASA TM-81146, March 1980.

⁶Hoh, R.H., Klein, R.H., and Johnson, W.A., "Development of an Integrated Configuration Management/Flight Director System for Piloted STOL Approaches," NASA CR-2883, Aug. 1977.

⁷Lebacqz, J.V. and Aiken, E.W., "A Flight Investigation of Control, Display, and Guidance Requirements for Decelerating Descending VTOL Instrument Transitions Using the X-22A Variable Stability Aircraft," Report AK-5336-F-1, Calspan Corp., Buffalo, NY, Sept. 1975.

⁸Lebacqz, J.V., Radford, R.C., and Beilman, J.L., "An Experimental Investigation of Control-Display Requirements for Jet-Lift VTOL Aircraft in the Terminal Area," NADC-76099-60, Naval Air Development Center, July 1978.

⁹Kelly J.R., Niessen, F.R., Thibodeaux, J.J., Yenni, K.R., and Garren, J.F. Jr., "Flight Investigation of Manual and Automatic VTOL Decelerating Instrument Approach Capability," NASA TN D-7524, July 1974.

¹⁰Niessen, F.R., Kelly, J.R., Garren, J.F. Jr., Yenni, K.R., and Person, L.H., "The Effect of Variations in Controls and Displays on Helicopter Instrument Approach Capability," NASA TN D-8385, Feb. 1977.

¹¹Merrick, V.K., "Simulation Evaluation of Two VTOL Control/Display Systems in IMC Approach and Shipboard Landing," NASA TM-85996, Dec. 1984.

¹²Farris, G.G., Merrick, V.K., and Gerdes, R.M., "Simulation Evaluation of Flight Controls and Display Concepts for VTOL Shipboard Operations," AIAA Paper 83-2173, Aug. 1983.

¹³Meyer, G. and Cicolani, L., "Application of Nonlinear System Inverses to Automatic Flight Control Design—System Concepts and Flight Evaluations," AGARDograph No. 251, July 1981.

¹⁴Meyer, G., "The Design of Exact Nonlinear Model Followers," *Joint Automatic Control Conference Proceedings*, IEEE, Charlottesville, VA, June 1981.

¹⁵Meyer, G., Su, R., and Hunt, L., "Application of Nonlinear Transformations to Automatic Control," *Automatic Control Conference Proceedings*, IEEE, Arlington, VA, June 1982.

¹⁶Franklin, J.A. and Hynes, C.S., "Flight Evaluation of Highly Augmented Controls and Electronic Displays for Precision Approach and Landing of Powered-Lift Aircraft," AIAA Paper 85-1944, Aug. 1985.

¹⁷Cochrane, J., Riddle, D., and Stevens, V., "Quiet Short-Haul Research Aircraft—The First Three Years of Flight Research," AIAA Paper 81-2625, Dec. 1981.

¹⁸McCracken, R., "Quiet Short-Haul Research Aircraft Familiarization Document," NASA TM-81149, Nov. 1979.

¹⁹Watson, D., "Quiet Short-Haul Research Airplane Mode Select Panel Functional Description," NASA TM-84243, May 1982.

²⁰Maier, R.E., "QSRA Performance Program User's Guide and Math Model Description," Document No. D340-10101, Boeing Commercial Airplane Co., Seattle, WA, Feb. 1979.

²¹Hynes, C.S., Scott, B.C., Martin, P.W., and Bryder, R.B., "Progress Toward Development of Civil Airworthiness Criteria for Powered-Lift Aircraft," NASA TM X-73, 124, May 1976.

²²Erzberger, H. and McLean, J.D., "Fuel-Conservative Guidance System for Powered-Lift Aircraft," *Journal of Guidance and Control*, Vol. 4, May-June 1981, pp. 253-261.

²³Franklin, J.A., Innis, R.C., Hardy, G.H., and Stephenson, J.D., "Design Criteria for Flightpath and Airspeed Control for the Approach and Landing of STOL Aircraft," NASA TP-1911, March 1982.

From the AIAA Progress in Astronautics and Aeronautics Series

SPACE SYSTEMS AND THEIR INTERACTIONS WITH EARTH'S SPACE ENVIRONMENT—v. 71

Edited by Henry B. Garrett and Charles P. Pike, Air Force Geophysics Laboratory

This volume presents a wide-ranging scientific examination of the many aspects of the interaction between space systems and the space environment, a subject of growing importance in view of the ever more complicated missions to be performed in space and in view of the ever growing intricacy of spacecraft systems. Among the many fascinating topics are such matters as: the changes in the upper atmosphere, in the ionosphere, in the plasmasphere, and in the magnetosphere, due to vapor or gas releases from large space vehicles; electrical charging of the spacecraft by action of solar radiation and by interaction with the ionosphere, and the subsequent effects of such accumulation; the effects of microwave beams on the ionosphere, including not only radiative heating but also electric breakdown of the surrounding gas; the creation of ionosphere "holes" and wakes by rapidly moving spacecraft; the occurrence of arcs and the effects of such arcing in orbital spacecraft; the effects on space systems of the radiation environment, etc. Included are discussions of the details of the space environment itself, e.g., the characteristics of the upper atmosphere and of the outer atmosphere at great distances from the Earth; and the diverse physical radiations prevalent in outer space, especially in Earth's magnetosphere. A subject as diverse as this necessarily is an interdisciplinary one. It is therefore expected that this volume, based mainly on invited papers, will prove of value.

Published in 1980, 737 pp., 6×9, illus., \$35.00 Mem., \$69.50 List

TO ORDER WRITE: Publications Order Dept., AIAA, 1633 Broadway, New York, N.Y. 10019